

Fracture of heterogeneous materials with continuous distributions of local breaking strengths

P. L. Leath

Department of Physics and Astronomy, Rutgers University, Piscataway, New Jersey 08855-0849

P. M. Duxbury*

Hochleistungsrechenzentrum and Institut für Festkörperforschung, Forschungszentrum Jülich, D-52425 Jülich, Germany

(Received 6 December 1993)

We develop a recursion-relation approach for the failure probability of heterogeneous networks with continuously distributed bond strengths and with local stress enhancements after bond failure. Current computational methods to solve these models scale as 2^n where n is sample size, while our method provides a rapidly converging sequence of approximations which scale algebraically with the sample size. The method is applied to systems with uniform and Weibull distributions of local bond-failure thresholds. We find that the characteristic feature which occurs when there is a continuous distribution of local breaking strengths is that, as a function of sample size, the failure probability $F_n(\sigma)$ shows a minimum at n_c , which deepens and moves to higher n as the external stress σ is reduced. At large n , there is a stable “weak-link” scaling form for the failure probability, in agreement with work by Harlow and Phoenix. For sufficiently large $n \gg n_c$, the failure probability is of double-exponential form, and the size effect is logarithmic. For small $n < n_c$, however, the low-stress tail of the failure probability appears to be of Weibull form with n -dependent parameters, and the size effect can be algebraic.

I. INTRODUCTION

Mechanical failure of a sufficiently large sample of a heterogeneous material consists of a crack nucleation process followed by the formation of an unstable crack and finally catastrophic failure. Traditional fracture mechanics bypasses the crack nucleation stage by postulating the existence of a crack and analyzing its consequences. Since fracture properties are determined by impurities, analysis of the nucleation of fracture is a problem in heterogeneous nucleation. As in most heterogeneous nucleation processes, significant sample-to-sample and configuration-to-configuration variability occurs in fracture strength and other fracture properties. For this reason a statistical analysis is often necessary, and in fracture this analysis is usually based on the Weibull and other extreme value distributions.¹

Understanding of crack nucleation and failure of heterogeneous materials has improved recently with the development of simple algorithms to simulate these processes in quasistatic loading.²⁻⁶ However it is difficult to reliably determine the scaling properties from these simulations, both because the algorithms are relatively slow, and because the scaling behavior is quite weak, so that many decades in sample size are required for a definitive analysis. A further problem with these simulations is that, in fracture, it is often the probability of failure that is of more interest than average properties such as the average fracture strength, and in particular, the “high-reliability” tail of the failure distribution is of most physical and engineering importance. Naturally, it is difficult to sample the high-reliability tail using conventional Monte Carlo methods. It is thus very important to develop a set of simple models which can be analyzed, either analytically or numerically, with precision to guide in the

analysis of the more complex models.

There is a long tradition in the use of simple models to analyze failure in heterogeneous materials. The majority of models are of mean-field type and ignore the stress enhancement near locally failed regions. These “democratic” or “equal-load-sharing” models are usually analytically solvable.⁷ Continuum versions of these mean-field models, which are often used to analyze the time to failure rather than the fracture strength, form an important branch of nonlinear continuum elastic theory called “continuum damage mechanics”.⁸ Rigorous treatment of the effect of local stress enhancements on crack nucleation has proven more difficult, and with the exception of the seminal work by Smith,⁹ Harlow and Phoenix,¹⁰⁻¹² and more recent work in the statistical physics community by us^{5,13} and Curtin and Scher,¹⁴ there are few reliable results. Although the solvable models are invariably one-dimensional, “fiber-bundle” models, they appear to contain many of the key scaling properties of more complex higher-dimensional models.

A key fiber-bundle model is one in which the local failure thresholds are drawn from continuous distributions, such as the Weibull and uniform distributions, and in which local stress enhancements occur after local failure. Harlow and Phoenix¹⁰ studied this model using a transition-matrix approach. In this paper we present a new recursion relation for this class of model and give detailed results for the average strength, the failure probability, and the distribution of stable crack sizes of fiber bundles with local load sharing and uniform and Weibull distributions of local failure thresholds.

The paper is arranged as follows. In Sec. II, we develop the recursion relations for the failure probability. In Sec. III, we present numerical results for the failure probability, average strength, and stable crack size distribu-

tions in the cases of uniform and Weibull distributions of local failure thresholds. Section IV contains a summary of the main results of the paper.

II. THE MODEL AND RECURSION FORMULAS FOR THE FAILURE PROBABILITY

The parallel-bar (fiber-bundle) model with a continuous distribution of bond failure thresholds is illustrated in Fig. 1. Prior to application of the applied stress [Fig. 1(a)], no bonds are broken and each of the bonds has a strength drawn from a distribution $f(\sigma')$. When a stress σ is applied, either some of the bonds fail until a stable crack structure is reached [Fig. 1(b)], or bond failure continues until the bundle fails completely. In the local-load-sharing model, the stress experienced by a surviving bond is given by

$$\sigma_k = \left[1 + \frac{k}{2} \right] \sigma, \tag{1}$$

where k is the number of failed bonds adjacent, on both sides, to a surviving bond [see Fig. 1(b)]. Although this load-sharing rule is idealized, it is similar to that occurring in composites and random networks (further justification can be found in Ref. 10).

We focus on calculating the probability $F(n, \sigma) = F_n$, that a bundle, or quasi-one-dimensional sample, of size n will fail when a stress σ is applied to the parallel-bar system. Often it is more convenient to work with the survival probability $S_n = 1 - F_n$. We develop recursion relations which relate F_n to the set $\{F_l, \text{with } l < n\}$. We have developed two distinct sets of recursion relations. The first is exact, but requires a computational effort which scales as $2^n - 1$. While the second is approximate, it scales algebraically with sample size and we show how it may be systematically improved. The approximate recursion relations are exact solutions to a set of simpler models, which in many cases contain the typical scaling behavior of the problem.

A. Exact recursion relation

It is simple to write down all of the configurations which survive in a sample of size n . In the following a 1 denotes a surviving fiber, while a 0 denotes a failed fiber. Then for fibers up to size 4, the survival configurations and their survival probabilities are listed in Table I (we have used reflection symmetry to reduce the number of distinct configurations). There are $2^n - 1$ survival configurations, and the one failure configuration 00...0 making a total of 2^n configurations on a sample of size n .

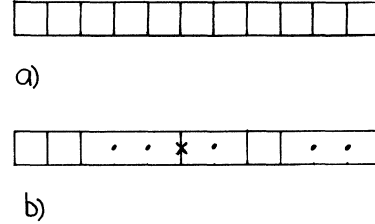


FIG. 1. (a) A parallel-bar system before fibers begin breaking; (b) a parallel-bar system after some fibers have broken. The lone fiber (LF) marked with an X, has load enhancement $k = 3$.

Each of these survival configurations is independent, so we can add their probabilities, $s(\text{configuration})$, to find the probability that a sample of size n survives,

$$S_n = \sum_{\text{configurations}} s(\text{configuration}). \tag{2}$$

It is also straightforward to write down the survival probability for any of the configurations in Table I and, for example,

$$s(0101) = F_1 W_2 F_1 W_1, \tag{3}$$

where we define

$$W_k = 1 - \int_0^{(1+k/2)\sigma} f(\sigma') d\sigma', \tag{4}$$

W_k is the probability that a fiber survives when it has k failed fibers adjacent it. Using this procedure, it is straightforward to complete Table I, and to calculate the failure probability of a sample of size n from $\{W_l \text{ and } F_l, l < n\}$. Harlow and Phoenix¹⁰ have developed a different method to calculate F_n , and we have analytically shown (to order $n = 4$) that our method gives the same result as theirs. Kuo and Phoenix¹² have labeled the survival configurations, in both the static failure (the case studied here) and the time-dependent failure problem, in the manner used here, but have not explicitly carried through the calculations in the way that we do here and in the next part of this section.

We have developed a computer algorithm to sum the $2^n - 1$ survival configurations of a sample of size n , and the results of these calculations will be presented in Sec. III. However, the exponential increase in the number of configurations occurring in the sum (2) restricts this algorithm to $n \approx 20$. To alleviate this problem, we have developed a more efficient recursion relation for F_n , and this we now describe.

TABLE I. Survival configurations and their survival probabilities.

Configurations (degeneracy)	Survival probabilities
1	W_0
11,10(2)	$W_0^2, 2W_1F_1$
111,110(2),101,100(2),010	$W_0^3, 2W_0W_1F_1, W_1F_1W_1, 2W_2F_2, F_1W_2F_1$
1111,1110(2),1101(2),1100(2),1010(2)	$W_0^4, 2W_0^2W_1F_1, 2W_0W_1F_1W_1, 2W_0W_2F_2, 2W_1F_1W_2F_1$
1001,0110,1000(2),0100(2)	$W_2F_2W_2, F_1W_2^2F_1, 2W_3F_3, 2F_1W_3F_2.$

B. Recursion relation using a generating-function technique

Our generating-function technique is based on the observation that any survival-configuration probability consists of products of independent probabilities of simpler subunits. The essential subunits and their generating functions are first defined, and then the generating function for the sum of probabilities of *all* survival

configurations is constructed from them.

Due to the nature of the load-sharing rule (1), it is useful to define a *lone fiber* (LF) to be a surviving fiber which is surrounded by failed fibers [e.g., the fiber marked with an *x* in Fig. 1(b)]. We then define $\{A\}$, to be the set of all survival configurations which contain only failed fibers *and* lone fibers, *and* are bracketed at both ends by lone fibers. The small *n* members of this set are

$$\{A\} = 101, 1001, 10001, \dots, 10101, 100101, 101001, \dots, 1010101, 10010101, \dots \tag{5}$$

A closely related set of configurations, $\{B\}$, we define to be the same set as $\{A\}$, with the exception that one (specified) end of the configuration must be failed. The small *n* members of this set (for the case where the left end is failed) are

$$\{B\} = 01, 001, 0001, \dots, 0101, 00101, 01001, \dots, 010101, 001010, \dots \tag{6}$$

There is a complimentary set to $\{B\}$ which has the same probability but which has the failed ending on the right. The generating functions for $\{B\}$ and its compliment are the same, so we do not distinguish between them. We also treat as special the set of configurations $\{C\}$ which is the same as $\{A\}$ except that *both* ends have failed. The small *n* members of this set are

$$\{C\} = 010, 0100, 0010, 01010, 001010, \dots \tag{7}$$

Finally, we also define $\{p\}$ the set of configurations which have no failed bonds

$$\{p\} = (.), 1, 11, 111, 1111, \dots \tag{8}$$

where $(.)$ is the empty set. Associated with these classes of survival configurations, we define the generating functions

$$A(z) = \sum_{n=3}^{\infty} A_n z^n,$$

$$B(z) = \sum_{n=2}^{\infty} B_n z^n,$$

and

$$C(z) = \sum_{n=3}^{\infty} C_n z^n,$$

where $A_n, B_n,$ and C_n are the sums, respectively, of the survival probabilities of the sets $\{A\}, \{B\},$ and $\{C\}$ of fixed sample size *n*. The generating function for the set $\{p\}$ may be evaluated immediately and we find

$$p(z) = \sum_{n=0}^{\infty} (W_0)^n z^n = \frac{1}{1 - W_0 z}. \tag{10}$$

Some study shows that the probabilities of all survival configurations are uniquely counted in the key generating function, $S(z)$

$$S(z) = C(z) + \frac{[1 + B(z)]p(z)[1 + B(z)]}{1 - p(z)A(z)}, \tag{11}$$

where

$$S(z) = \sum_{n=0}^{\infty} S_n z^n. \tag{12}$$

To see how this arises, it is necessary to replace the generating functions in Eq. (11) with the survival configuration to which each term refers, and then show that expression (11) reproduces all possible survival configurations. An example (for *n*=3) is given in the Appendix. Since we have the identity

$$F_n = 1 - S_n, \tag{13}$$

we also have the generating-function identity

$$F(z) = \sum_{n=0}^{\infty} F_n z^n = \frac{1}{1 - z} - S(z). \tag{14}$$

We note also that $F_0 = 0$ and $S_0 = 1$. Combining (10), (11), and (14), we get the identity

$$(1 - z)(1 + B)^2 - (1 - W_0 z - A)[1 - (1 - z)(F + C)] = 0. \tag{15}$$

We then expand this identity using definitions (9) and (14), and setting the coefficient of the z^n term in this expression to zero yields the recursion relation

$$F_n + C_n = (1 + W_0)(F_{n-1} + C_{n-1}) - W_0(F_{n-2} + C_{n-2}) - 2B_n + 2B_{n-1} - A_n + F_1 A_{n-1} - B_2 B_{n-2} + \sum_{m=1}^{n-4} \{B_{m+1}(B_{n-m-2} - B_{n-m-1}) + A_{m+2}[(F_{n-m-2} + C_{n-m-2}) - (F_{n-m-3} + C_{n-m-3})]\}. \tag{16}$$

To implement this recursion relation, we need expressions for the survival probabilities $A_n, B_n,$ and C_n . We are able to write down expressions for $A_n, B_n,$ and C_n as a series in the number of lone fibers (excluding end fibers) occurring in a survival configuration. These series with terms up to two lone fibers explicitly listed are as follows [typical survival

configurations considered are contained in Eqs. (5)–(7)]:

$$A_n = W_{n-2}^2 F_{n-2} + \sum_{l_1=1}^{n-4} W_{l_1} W_{n-3} W_{n-l_1-3} F_{l_1} F_{n-l_1-3} \\ + \sum_{l_1=1}^{n-6} \sum_{l_2=1}^{n-l_1-5} W_{l_1} W_{l_1+l_2} W_{n-l_1-4} W_{n-l_1-l_2-4} F_{l_1} F_{l_2} F_{n-l_1-l_2-4} + \cdots, \quad (17)$$

$$B_n = W_{n-1} F_{n-1} + \sum_{l_1=1}^{n-3} W_{n-2} W_{n-l_1-2} F_{l_1} F_{n-l_1-2} \\ + \sum_{l_1=1}^{n-5} \sum_{l_2=1}^{n-l_1-4} W_{l_1+l_2} W_{n-l_1-3} W_{n-l_1-l_2-3} F_{l_1} F_{l_2} F_{n-l_1-l_2-3} + \cdots, \quad (18)$$

and

$$C_n = \sum_{l_1=1}^{n-2} W_{n-1} F_{l_1} F_{n-l_1-1} + \sum_{l_1=1}^{n-4} \sum_{l_2=1}^{n-l_1-3} W_{l_1+l_2} W_{n-l_1-2} F_{l_1} F_{l_2} F_{n-l_1-l_2-2} + \cdots. \quad (19)$$

Equations (16)–(19) are the complete set of recursion relations for the failure probability. It is computationally very expensive to take Eqs. (17)–(19) to arbitrary order in the number of lone fibers, although it is faster to solve the problem exactly this way than using the configuration-counting method described earlier in this section.

However an important feature of Eqs. (17)–(19) is that they allow us to systematically include successively higher-order lone-fiber configurations. The i -lone-fiber (NLF= i) approximation is done by neglecting all the terms in A_n , B_n , and C_n [as given by Eqs. (17)–(19)] which have more than $(i+1)$ products of F 's in them. This sequence of approximations, in which we take increasing numbers of lone fibers into calculations, provide a *uniformly converging sequence of upper bounds* to the exact failure probability, since we are systematically increasing the number of survival configurations. In fact, in the simpler problem of diluted networks or fiber bundles, Harlow and Phoenix¹¹ found that taking the terms up to order NLF=2 lone fibers provided asymptotically exact results for the bundle failure probability. In the next section we study the recursion relation (16) up to order NLF=2 and compare the results with the exact method described earlier. Before proceeding to these calculations, it is useful to illustrate the survival configurations which are included at each order in our NLF approximations to A_n , B_n , and C_n . We illustrate using $\{A\}$, and consider for illustration the three configurations

$$\begin{aligned} X1 &= 10011011011101, \\ X2 &= 10010011000101, \\ X3 &= 10010001011101. \end{aligned} \quad (20)$$

When no lone fibers (NLF=0) are considered in the calculations, all surviving fibers (other than those on the ends of the string) must have at least one adjacent surviving fiber, thus $X1$ is included, but not $X2$ or $X3$. When one lone fiber is allowed (NLF=1) in the calculations, $X1$ and $X2$ are included but not $X3$. Finally, when NLF=2

all three configurations in (20) are included in the calculations, while a configuration such as 101010101 is not (it has a string of three sequential lone fibers). Even the leading-order model (NLF=0) is very interesting, and is analogous to the *single-cluster load-sharing model* solved for the case of random dilution.^{5,13} In that case this simple model contains much of the essential scaling properties of the model, and we will see that low-order lone-fiber models seem numerically to contain the essential physics of the systems studied here.

III. NUMERICAL RESULTS

We calculate the failure probability F_n recursively from Eqs. (16)–(19), using the load-sharing rule (1), and Eq. (4) for W_n . The local bond-failure probabilities we use are the uniform distribution with differential probability,

$$f_u(\sigma) = \frac{1}{W} \quad \text{if } 0 \leq \sigma \leq W$$

and

$$f_u = 0 \quad \text{otherwise.}$$

The only parameter in the uniform distribution is the width W . In order to compare with prior work such as that by Harlow and Phoenix,¹⁰ we also use the local Weibull distribution with cumulative probability

$$\begin{aligned} c_\omega(\sigma) &= \int_0^\sigma f_\omega(\sigma') d\sigma' \\ &= 1 - \exp \left[- \left(\frac{\sigma}{\sigma_s} \right)^m \right]. \end{aligned} \quad (22)$$

This distribution has two parameters, σ_s the scale strength, which sets the size of the typical strength in the distribution, and m the Weibull modulus, which determines the scatter in the distribution of bond strengths. In both of these cases it very simple to evaluate W_n from Eq. (4). From Table I it is straightforward to write down

$$F_1 = 1 - W_0$$

and

$$F_2 = 1 - W_0^2 - 2W_1F_1. \quad (23)$$

Then we either use the configuration-counting method of the first part of Sec. II or the recursion relations Eqs. (16)–(19) of Sec. II to find higher order F_n . When using the recursion relation method, we are able to include successively higher-order terms in Eqs. (17)–(19). When no lone-fiber configurations are included (NLF=0), we include the first term in Eqs. (17) and (18). When a single lone-fiber string is allowed (NLF=1), we include the first two terms in (17) and (18) and the first term in (19). Finally, when a string of two lone fibers is allowed, NLF=2, we include the first three terms in (17) and (18) and the first two terms in (19). As stated at the end of Sec. II, this gives us the first three terms in a converging sequence of upper bounds on F_n . Using the exact method we are able to calculate F_n to order $n=20$ in about a minute CPU on a Sun Workstation. Using the recursion method, we are able to calculate F_n to order $n=150$ for NLF=2, and order $n=1500$ for NLF=1 in about a minute CPU on a Sun Workstation. Storage requirements are minimal, and improvements by factors of 2 or so could be easily achieved in optimized programs.

A. Uniform distribution

Results for $F_n(\sigma)$ for the uniform distribution with $n=20$ are presented in Fig. 2(a). Here we have calculated the failure probability exactly, and compare it with the approximations NLF=0,1,2. The results for NLF=2 are coincident with the exact result to the resolution of this graph, although in the lower tail, there are significant deviations (see below). In Fig. 2(b), we present results for NLF=1, for $n=15, 150, 1500$ to illustrate the variation in the failure probability with sample size. It is seen that the mean of the probability distribution moves toward $\sigma/W=0$, and becomes sharper (less fluctuations) with increasing n . Harlow and Phoenix¹⁰ have shown that at large sample size, F_n should approach the *weak-link* scaling form

$$1 - F_n \approx [1 - f_1(\sigma)]^n. \quad (24)$$

This is called weak-link statistics, as the survival of a sequence of n links each of which is independent and has survival probability $s(\sigma)$ is $S_n = [s(\sigma)]^n$. Conversion from survival probability to failure probability gives exactly Eq. (24). It is surprising and nontrivial that the weak-link form (24) should apply in problems with correlated bond-breaking schemes. One way to test for convergence of data such as Fig. 2(b) to Eq. (24) is to plot the

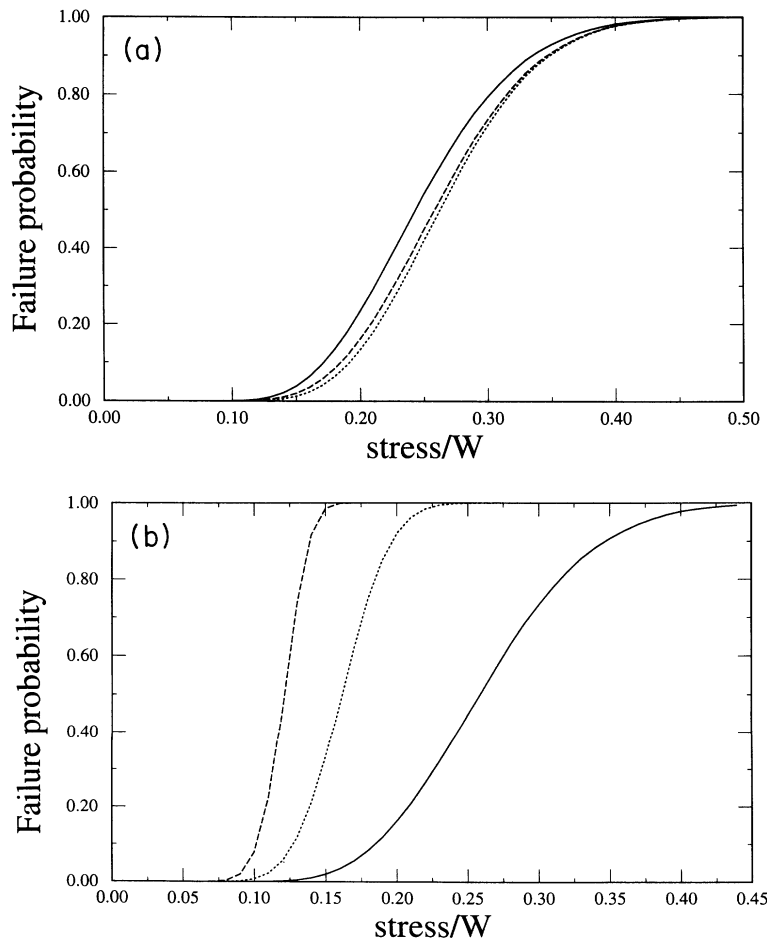


FIG. 2. (a) The failure probability F_n of an $n=20$ system with a uniform distribution of fiber thresholds: the exact result (---), the NLF=0 approximation (—), and the NLF=1 approximation (---). The NLF=2 approximation is coincident with the exact result to the resolution of this figure. (b) The failure probability within the NLF=1 approximation for $n=15$ (—), $n=150$ (---), and $n=1500$ (---).

quantity $X = \ln[-\ln(1 - F_n)/n]$ against some function of σ . Although this is not the simplest function to test Eq. (24), it has the advantage of also testing predictions for the form of $f_l(\sigma)$ appearing in Eq. (24). In Figs. 3(a) and 3(b), we present plots of X versus two functions of σ/W . From Fig. 3(a) it is seen that for n sufficiently large, the data fall on a common line, and hence that Eq. (24) is valid in this limit. It is also seen from this figure that for $n = 15$, the uniform distribution is far from achieving the weak-link form, but that for $n = 150$ the weak-link form is accurate. It is evident that although there are significant quantitative differences between the NLF=1 and 2 cases, the general trends are very similar for these two approximations. Figure 3(a) also provides a test of the Weibull form for the stable limiting distribution. If the Weibull form were correct, then the low-stress tail of Fig. 3(a) should be a straight line. For $n = 15$, the line does appear to be straight for $\ln(\sigma/W) < 2.3$, indicating a region in which the Weibull form is useful. In fact, for each value of n , it seems that the Weibull plot becomes straight for sufficiently low stress, but that region moves to lower and lower values of stress as n increases, and the asymptotic straight line (Weibull fit) has parameters which are highly sample size dependent.

A test of the double-exponential form for the same data for $F_n(\sigma)$, suggested from previous work on the

models with random dilution [$f_l(\sigma) \sim \exp(-a/\sigma)$, see Refs. 5 and 13] is presented in Fig. 3(b). The data are nearly a straight line for $n = 150$, with slight curvature. The slight curvature suggests that a preexponential factor may be required, such as $f_l(\sigma) \sim \sigma^\alpha \exp(-a/\sigma)$, which has been found previously for $\alpha = -1$, in models with random dilution.¹³ The $n = 15$ data are straight for high stress, but curves away sharply at low stress as the Weibull-like behavior takes over.

More information about the behavior of F_n as a function of n is presented in Fig. 4. Figure 4(a) shows the behavior of F_n as a function of n at $\sigma/W = 0.1$, which is in the low-stress tail of Fig. 3. Here it is seen that there is a striking nonmonotonic behavior of the failure probability as a function of sample size. The failure probability at the minimum of Fig. 4(a) is 4 orders of magnitude lower than that of a single bond. Qualitatively the origin of this effect is that for a specified disorder, there is a tendency toward crack blocking by strong bonds, and a tendency toward crack propagation when a large cluster of defects arises. At small external stresses, the critical defect size for unstable crack propagation is large, and hence crack blocking is very significant. For samples of a given size n , the external stress σ can be sufficiently small that it is unlikely that a crack of the critical size, i.e., an unstoppable crack, exists in the sample. If bond breaking

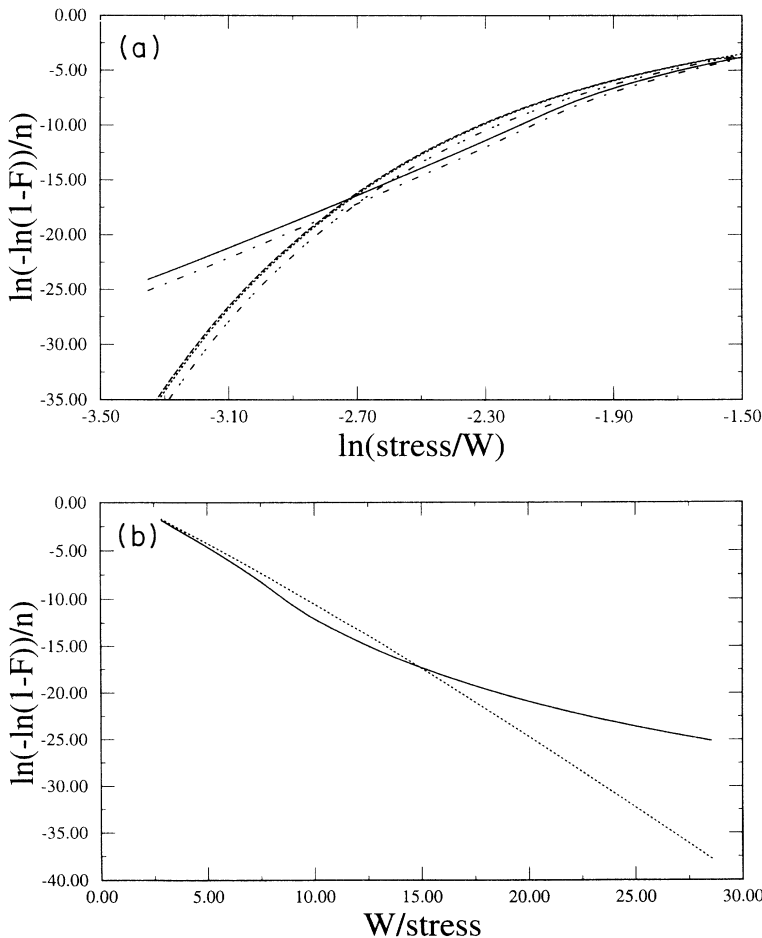


FIG. 3. A test of the weak-link hypothesis [Eq. (24) of the text] for the uniform distribution. (a) A test of the Weibull stable limiting form, for $n=15$ with NLF=1 (—) and NLF=2 (---); $n=150$ with NLF=1 (-.-) and NLF=2 (-.-.-); and $n=1500$ with NLF=1 (-.-.-). (b) the $n=15$, NLF = 2 data (—) and the $n=150$, NLF=2 data (---) from (a), to test for the double-exponential distribution.

is completely random, the probability that a sample of size n will fail at stress σ/W is $F_n \sim (\sigma/W)^n$. This probability is a strongly *decreasing* function of system size, which explains why, at small applied stress, the graphs of Fig. 4 are initially strongly decreasing functions of sample size n . In this region, failure occurs by the percolation of cracks. It is in this region that Weibull-type behavior is seen with n -independent parameters. However, in a large system, an especially weak or highly stressed

part of the system becomes unstable, develops a supercritical crack which is unstoppable and catastrophic failure occurs. The minimum of graphs such as Fig. 4(a) then defines a critical sample size n_c . For samples larger than the critical size, the probability of failure increases, as the likelihood of nucleating a critical defect becomes large. As shown in Fig. 4(b), the critical sample size gets larger as the applied stress level is made smaller, and at the same time, the minimum in the F_n versus n curve

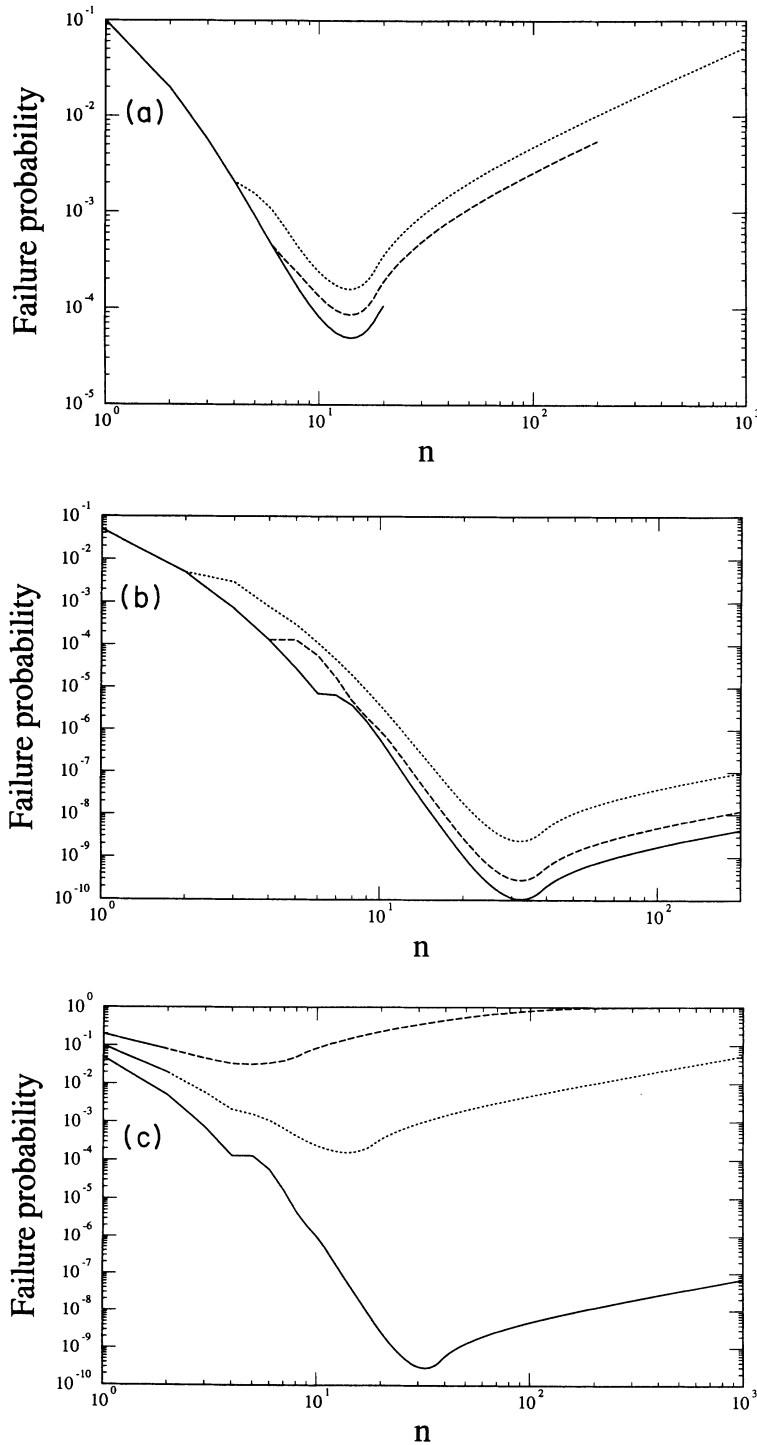


FIG. 4. The failure probability F_n for the case of the uniform distribution, as a function of system size n . (a) $\sigma/W=0.1$ the exact result (—), $NL=1$ (---), and $NL=2$ (· · ·); (b) $\sigma/W=0.05$ for $NL=0$ (· · ·), $NL=1$ (---), $NL=2$ (—), and (c) results for $NL=1$ and $\sigma/W=0.2$ (---), $\sigma/W=0.1$ (· · ·), and $\sigma/W=0.05$ (—).

grows deeper. At $\sigma/W=0.05$ the minimum is close to $n=32$, and the minimum in F_n is nearly 9 orders of magnitude lower than the single-bond failure probability. It is seen from Figs. 4(a) and 4(b) that the NLF=1 and 2 approximations do not precisely determine the value of F_n in this regime, although the critical sample size n_c is in nearly the correct position even for NLF=0. As seen in Fig. 4(c), the depth of the minimum in F_n grows weaker as σ/W increases, and we find that F_n becomes monotonically increasing in n when σ/W exceeds a critical value of about 0.5. In this case, the critical-crack size is zero and the sample is in the brittle regime in the language of Khang *et al.*² It would be interesting to follow the behavior of n_c with $\sigma/W \rightarrow 0$, although the fact that the minimum in F_n becomes extremely deep makes this a difficult numerical task. However, there is a simple way in which to estimate the behavior of the critical sample size, as illustrated by the discussion below.

It is possible to calculate the (non-normalized) number of cracks of size l which are stable from the expression

$$N_l \sim W_l^2 F_l. \tag{25}$$

This is the probability that a region of size l has failed, multiplied by the probability that the two bonds at the ends of the crack survive. It does not separately count clusters with lone fibers in their interior. Double-logarithmic plots of N_l against l are presented in Fig. 5. It is clear that this stable crack-size distribution is not algebraic in this range, and a log-linear plot also shows it is not exponential. There is clearly a crack size above which no stable cracks can occur, and for the uniform distribution this critical crack size is certainly less than or equal to the point at which W_n goes to zero. This crack size leads to a cutoff in the curves of Fig. 5 and is responsible for the sharp downward curvature in the tail of the plots in Fig. 5. An estimate of the critical sample size for the uniform distribution is then

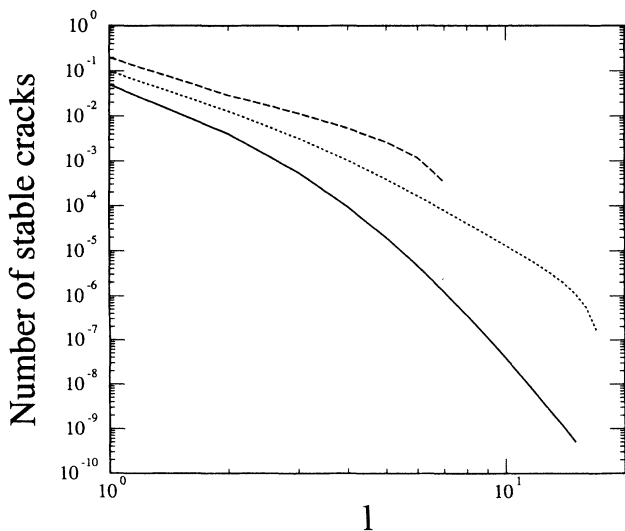


FIG. 5. The number of stable cracks (non-normalized), N_l , for $\sigma/W=0.05$ (—), $\sigma/W=0.1$ (---), and $\sigma/W=0.2$ (- - -).

$$1 - \frac{(n_{ca} + 2)\sigma}{2W} = 0. \tag{26}$$

This gives

$$n_{ca} = \frac{2W}{\sigma} - 2. \tag{27}$$

Note that although $n_{ca} \neq n_c$ as found from the minimum in F_n of Fig. 4, it is close to and a rather good upper bound on those minima.

The average strength, $\bar{\sigma}$, of the fiber bundles is easily calculated from $F_n(\sigma)$. Here we do two calculations, the first for a single-fiber bundle, and the second for a chain of n fiber bundles. When n fiber bundles are arranged in series or in a chain, so that each of the bundles is in-

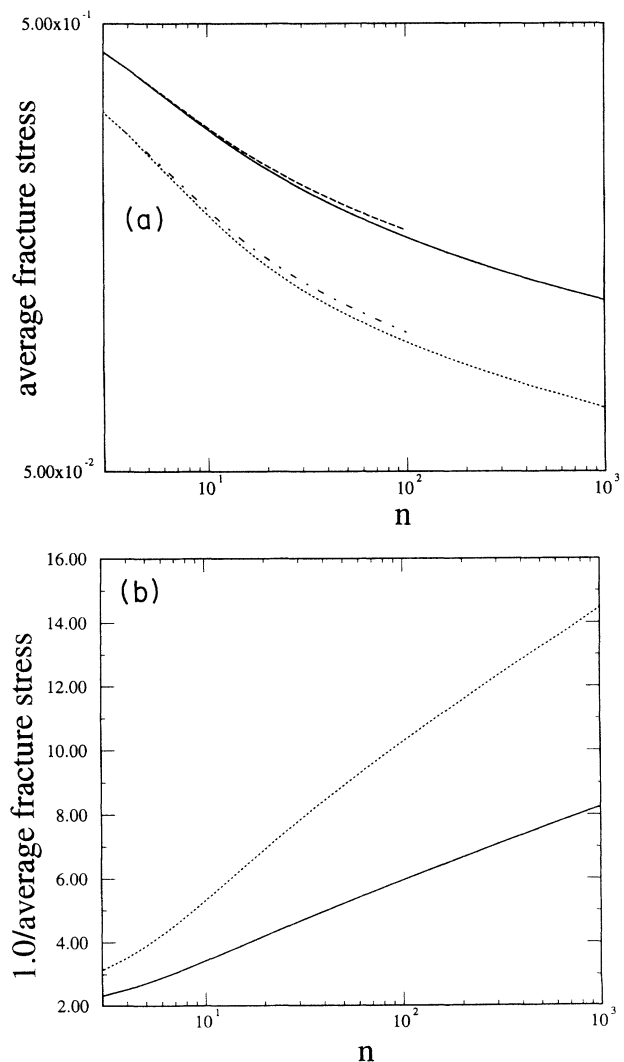


FIG. 6. The average fracture stress $\bar{\sigma}$ as a function of sample size for the uniform distribution. (a) for NLF=1 and a single-fiber bundle (—), for NLF=2 and a single-fiber bundle (---); for NLF=1 and a series combination of n fiber bundles (- - -), for NLF=2 and a series combination of n fiber bundles (· · ·). (b) A test of a logarithmic size effect in average strength, data for NLF=1 and a single-fiber bundle (—), and for NLF=1 and series combination of n fiber bundles (- - -).

dependent, the weak-line rule is exact, so we have

$$1 - G_{nn} = [1 - F_n]^n \sim [1 - f_l(\sigma)]^{n^2}. \quad (28)$$

Using G_{nn} , we calculate the average strength of $n \times n$ lattices. The results are presented in Fig. 6, in which we plot the data on a log-log graph to test for the behavior $\bar{\sigma} \sim 1/L^x$, as claimed in Ref. 3, where it is suggested that $x \sim 0.25$. It is seen that this algebraic form does not fit the data well. In Fig. 6(b), we plot $1/\bar{\sigma}$ to test the prediction that, up to $\log(\log)$ corrections, $\bar{\sigma} \sim 1/(1 + k \ln L)$ as argued by Duxbury and Kim.¹⁵ Earlier work by Smith⁹ suggested $\bar{\sigma} \sim 1/\ln L$ (similar arguments were also used by Khang *et al.*²). Figure 6(b) shows that the logarithmic form provides a better representation of the data than does the algebraic one except for very small values of n . The size effect is very weak, and it is not surprising that an algebraic fit with $x \sim \frac{1}{4}$ provides a reasonable fit to the data over a couple of decades in sample size. It is clear that attempts to find the scaling laws of fracture from simulations on small lattices (even lattices of up to 100×100) may not give the correct asymptotic trends, and that analytic results are essential to guide in the analysis of simulations.

B. Weibull distribution

Since the Weibull distribution has been so broadly applied and since it has no strict upper cutoff, it is of interest to see how our method performs in this case. We first present results to test whether the hypothesis of a stable, limiting weak-link distribution (24) is valid for this type of disorder. The results for a typical practical case $m=5$ are presented in Fig. 7. It is seen from this figure that except in the very high-reliability tail, the stable limiting distribution is achieved for $NLF=1$ and $n < 100$. We also present this figure in order to check consistency with the transition-matrix method of Harlow and Phoenix (see Fig. 3 of Ref. 10). Their method with $k \sim 10$ provides a similar convergence to the stable limiting distribution as that seen in Fig. 7(a), and provides a useful check on our method. It is seen from Fig. 7(a) that the limiting distribution is again not of Weibull form. In Fig. 7(b), we present a test of the double-exponential form, which is seen to be almost linear in the high-reliability tail. Again, we suggest that the double-exponential form with an algebraic prefactor is a very good way to analyze data such as Fig. 7, although in many practical situations, the experimental data are not good enough to resolve these subtleties.

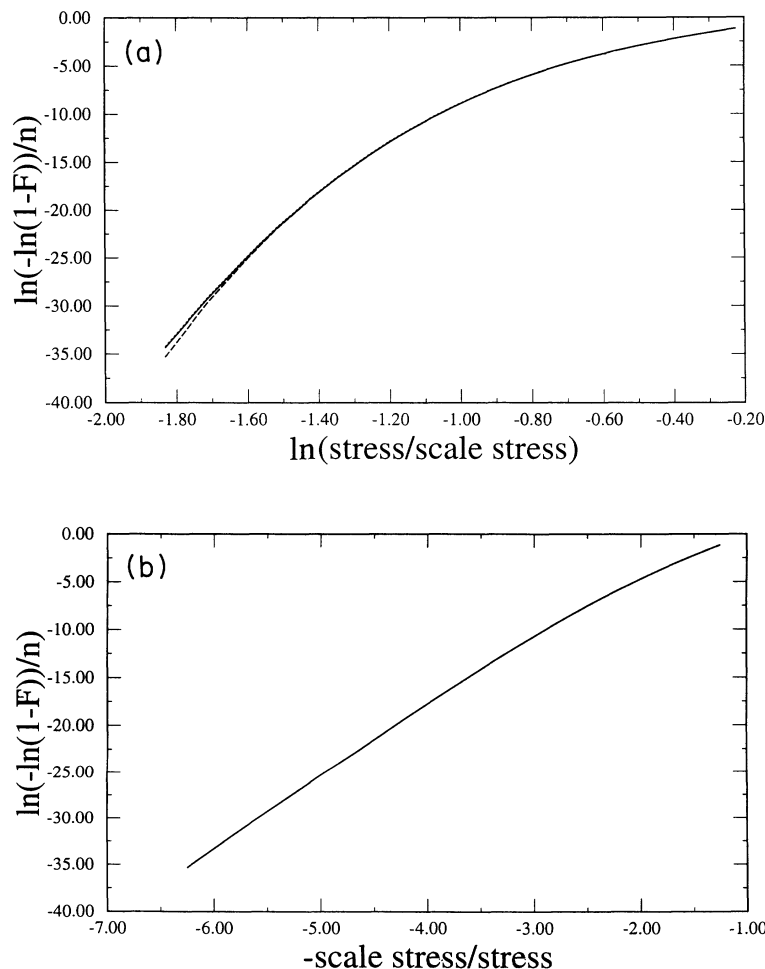


FIG. 7. A test of convergence to the weak-link scaling form (24) for the Weibull distribution with $m=5.0$. (a) Data for $NLF=1$ and $n=100$ (—) and $n=1000$ (---), and for $NLF=2$ and $n=100$ (---) on a Weibull plot. (b) Data for $NLF=2$ and $n=100$ to test for double-exponential scaling (—).

As in the uniform distribution case F_n for the local Weibull distribution is not monotonic in n and shows a striking minimum at a critical value of n . In Fig. 8(a), we show for $m=2$ and $\sigma/\sigma_s=0.2$ that NLF=2 provides an even better approximation to the depth and location of the probability minimum than it did in the uniform distribution case. As in the uniform distribution case, the minimum grows deeper as the stress is reduced [see Fig. 8(b)]. The small NLF approximations become more accurate as m increases [see Fig. 8(c)], and even at $m=5$,

the NLF=1 approximation is sufficiently accurate for most purposes. We observe that the sharper the distribution of local bond-failure thresholds, the more accurate are the NLF=1 and 2 approximations. In general, we expect that the failure probability of models with a well-defined peak in the distribution of bond-breaking strengths will be accurately estimated by using low-order NLF approximations. In fact, the uniform distribution is one of the most challenging cases for these approximations.

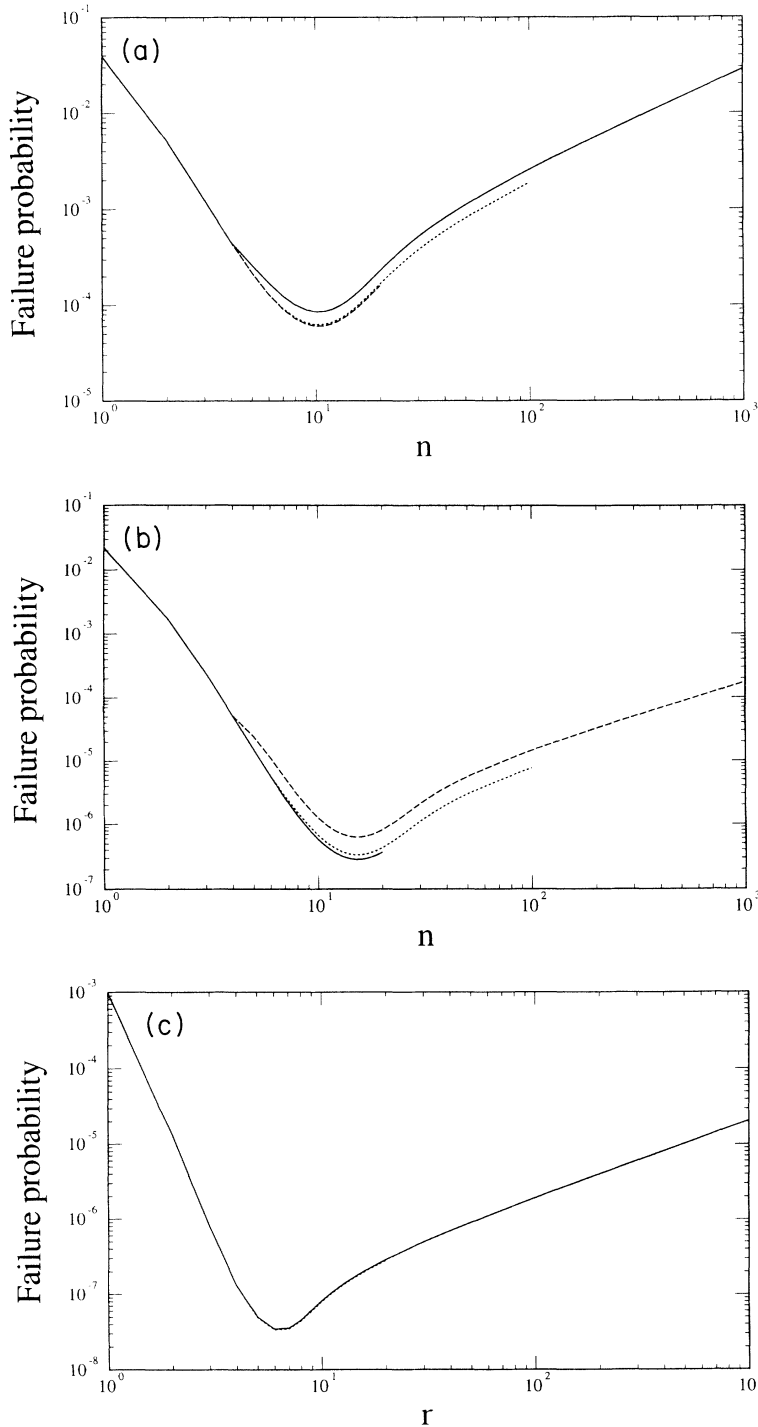


FIG. 8. The failure probability of the Weibull distribution as a function of sample size showing the deep minimum at a critical value of n . (a) Data for $m=2$, $\sigma/\sigma_s=0.2$, and NLF=1 (—), NLF=2 (---), and the exact result (---). (b) Data for $m=2$ and $\sigma/\sigma_s=0.15$ for NLF=1 (---), NLF=2 (---), and the exact result (—). (c) Data for $m=5.0$, $\sigma/\sigma_s=0.25$ for NLF=1 (—) and the exact result (---).

Finally, we have calculated the average strength of Weibull systems with $m=5$, and the results are present in Fig. 9. In the Weibull case, the larger m models are expected to show a logarithmic size effect,⁹ although the amplitude of the effect is weaker for larger m . Since there is a downward curvature in the plot of Fig. 9(b) the size effect is slightly weaker than logarithmic, but it is certainly inconsistent with an algebraic size effect at large n .

IV. SUMMARY

We have presented a new method to analyze the failure probability, crack-size distribution, and average strength of simple models of fracture with local load sharing. Simple transcription of variables (e.g., stress \rightarrow current, in the random-fuse case) makes these models also relevant to the behavior of the random fuse, superconducting, and dielectric models. The recursion-relation method is particularly powerful as it provides a converging sequence of upper bounds on the failure probability, and a converging sequence of lower bounds on the average strength. In many cases, these bounds are numerically essentially exact even for low-order approximations in the number of lone-fiber configurations (NLF's) included. The recursion algorithm is algebraic in sample size, in

contrast to a full solution which scales exponentially as 2^n . In addition, the fact that the failure probability is calculated directly allows this method to be used in the very important, high-reliability tail of the failure distribution, a regime which is inaccessible to direct numerical simulations.

We have applied our new algorithm to single-fiber bundles and to chains of fiber bundles or networks, with local-load sharing and we have used both the uniform and Weibull distributions of local-failure thresholds. The qualitative behavior is the same for both classes of disorder thresholds, although the approximations are better when the distribution is sharper, and our main results are as follows.

(1) There is a stable limiting *weak-link* [see Eq. (24)] distribution in the failure probability [see Figs. 3(a) and 7(a)], as first demonstrated by Harlow and Phoenix.¹⁰ A double-exponential distribution provides a better parametrization of the data than a simple Weibull (see Figs. 3 and 7), for large samples, although an n -dependent Weibull distribution works well for small samples and in the low stress tail.

(2) There is a deep minimum in the failure probability as a function of sample size (see Figs. 4 and 8), implying that there is an optimal size in the design of materials and structures with disordered microstructures if that is

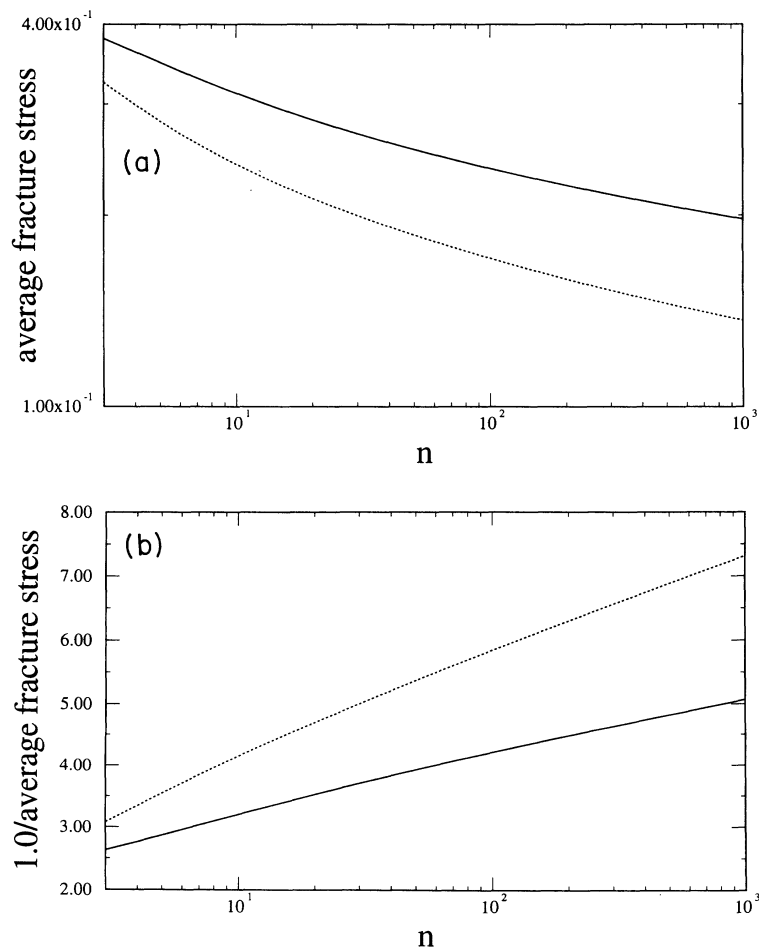


FIG. 9. The size effect in average strength for the Weibull distribution with $m=5.0$. (a) A log-log plot to test for algebraic scaling with $NLF=1$ and for a single-fiber bundle (—), and for a series combination of n fiber bundles (---). (b) Same data as for (a), but plotted to test a logarithmic size effect.

possible. The optimal system size becomes larger when the applied stress is smaller, and when the distribution of initial disorder is broader.

(3) For large sample sizes n , the size effect in fracture strength is slightly weaker than simple logarithmic but appears to be inconsistent with the algebraic scaling found in Ref. 3, but in agreement with arguments made by Smith⁹ and Duxbury and Kim.¹⁵ One must, however, be aware that the models studied here do not allow crack deflection, a process which certainly does occur in many higher-dimensional models, and the local load-sharing rule does not consider long-range strain fields. It is im-

portant to assess these effects before one can definitively claim to understand the analogous $d=2$ and 3 electrical and spring networks. Nevertheless, there is growing evidence that the models here provide an accurate picture of the dominant form of scaling at large sample size for a broad range of models and for a broad range of initial heterogeneity.

APPENDIX

Survival configurations to order $n=3$ may be generated from [see Eq. (11)] of text,

$$\{S\} = 010 + (. + 01 + 001) \frac{(. + 1 + 11 + 111)}{-(. + 1 + 11 + 111)(101)} (. + 10 + 100). \quad (\text{A1})$$

Here a (.) refers to the absence of any contribution to the configuration from that bracket. On expanding the denominator in a series expansion, it is seen that the right-hand side of (29) reproduces all survival configurations to order $n=3$. In order that the *probabilities* of survival can be decomposed in the same way as the configurations themselves, we must *not* break any vacant clusters, or at any places at which a vacant cluster meets a fiber (i.e., we cannot break a 00 segment at its center, and we cannot break a 01 segment). We can however break a segment 11, as the survival probabilities in this case are simple products. For example,

$$s(001001100010) = s(001001)s(100010). \quad (\text{A2})$$

This sort of decomposition has been discussed before by Kuo and Phoenix.¹² It is seen that this result also relies on the fact that the load-sharing rule Eq. (1) only applies to the bonds at the ends of vacant clusters. If the load sharing is to farther neighbors, the decomposition (30) is not valid in its present form, although generalizations to

include limited-range load sharing are possible. Despite this, the recursion method described in Sec. II of the text is still very general, as it applies to any load-sharing rule [i.e., one can replace (1), by exponential, or more general algebraic laws], and to any distribution of local-failure thresholds.

ACKNOWLEDGMENTS

P.L.L. thanks the Physics/Astronomy Department at Michigan State University and the Department of Theoretical Physics at Oxford University for their hospitality during his stay there. P.M.D. acknowledges the support of the DOE under Grant No. DE-FG02-90ER45418. P.M.D. was also supported by the Alexander von Humboldt Foundation at the IFF-Forschungszentrum Jülich. This assistance and the hospitality of the HLRZ at the Forschungszentrum Jülich are also gratefully acknowledged.

*Permanent address: Department of Physics and Astronomy and Center for Fundamental Materials Research, Michigan State University, East Lansing, MI 48824-1116.

¹W. Weibull, *J. Appl. Mech.* **18**, 293 (1951); E. J. Gumbel, *Statistics of Extremes* (Columbia University Press, New York, 1958); A. de S. Jayatilaka, *Fracture of Engineering Brittle Materials* (Applied Science, London, 1979).

²L. de Arcangelis, S. Redner, and H. J. Herrmann, *J. Phys. Lett.* **46**, L585 (1985); B. Khang, G. G. Batrouni, S. Redner, L. de Arcangelis, and H. J. Herrmann, *Phys. Rev. B* **37**, 7625 (1988).

³H. J. Herrmann, A. Hansen, and S. Roux, *Phys. Rev. B* **39**, 637 (1989); L. de Arcangelis and H. J. Herrmann, *ibid.* **39**, 2678 (1989); A. Hansen, S. Roux, and H. J. Herrmann, *J. Phys. (Paris)* **50**, 733 (1989); A. Hansen, E. L. Henrichsen, and S. Roux, *Phys. Rev. B* **43**, 665 (1991).

⁴M. Sahimi and J. D. Goddard, *Phys. Rev. B* **33**, 7848 (1986); S. Arbabi and M. Sahimi, *ibid.* **41**, 772 (1990); M. Sahimi and S. Arbabi, *ibid.* **47**, 713 (1993).

⁵P. M. Duxbury, P. D. Beale, and P. L. Leath, *Phys. Rev. Lett.*

57, 1052 (1986); P. M. Duxbury, P. L. Leath, and P. D. Beale, *Phys. Rev. B* **36**, 367 (1987); P. M. Duxbury and P. L. Leath, *J. Phys. A* **20**, L411 (1987).

⁶P. D. Beale and D. J. Srolovitz, *Phys. Rev. B* **37**, 5500 (1988); P. Meakin, *Science* **252**, 226 (1991); S. J. D. Cox and L. Pater-son, *Phys. Rev. B* **40**, 4690 (1989).

⁷F. T. Peirce, *J. Textile Inst.* **17**, 355 (1926); H. E. Daniels, *Proc. R. Soc. London, Ser. A* **183**, 405 (1945); L. N. McCartney and R. L. Smith, *J. Appl. Mech.* **50**, 601 (1983); S. L. Phoenix and R. Raj, *Act. Metall. Mater.* **40**, 2813 (1992); W. A. Curtin, *J. Am. Ceram. Soc.* **74**, 2837 (1991).

⁸*Continuum Damage Mechanics Theory and Applications*, edited by D. Krajcinovic and J. Lemaitre (Springer, New York, 1987).

⁹R. L. Smith, *Proc. R. Soc. London, Ser. A* **372**, 539 (1980); **382**, 179 (1982); *Adv. Appl. Prob.* **15**, 304 (1983).

¹⁰D. G. Harlow and S. L. Phoenix, *Int. J. Fracture* **17**, 601 (1981).

¹¹D. G. Harlow, *Proc. R. Soc. London, Ser. A* **397**, 211 (1985); D. G. Harlow and S. L. Phoenix, *J. Mech. Phys. Solids* **39**,

- 173 (1991).
- ¹²S. L. Phoenix and L. J. Tierney, *Eng. Fract. Mech.* **18**, 193 (1983); C. C. Kuo and S. L. Phoenix, *J. Appl. Prob.* **24**, 137 (1987).
- ¹³P. M. Duxbury and P. L. Leath, *Phys. Rev. B* **49**, 12 676 (1994).
- ¹⁴W. A. Curtin and H. Scher, *Phys. Rev. Lett.* **67**, 2457 (1991); W. A. Curtin and H. Scher, *Phys. Rev. B* **45**, 2620 (1992).
- ¹⁵P. M. Duxbury and S. G. Kim, *Mechanical Properties of Porous and Cellular Materials*, edited by D. Green, K. Sieradzki, and L. J. Gibson, *MRS Symposia Proceedings No. 207* (Materials Research Society, Pittsburgh, 1991), p. 179.